Hindawi
International Journal of Antennas and Propagation
Volume 2017, Article ID 2823565, 7 pages
https://doi.org/10.1155/2017/2823565

Research Article

A Novel *L*-Shape Ultra Wideband Chipless Radio-Frequency Identification Tag

Khaled Issa,[1] Muhammad A. Ashraf,[1] Mohammed R. AlShareef,[2] Hatim Behairy,[2] Saleh Alshebeili,[1] and Habib Fathallah[1,3]

[1]*KACST-TIC in Radio Frequency and Photonics for the e-Society (RFTONICS), Electrical Engineering Department, King Saud University, Riyadh, Saudi Arabia*
[2]*National Center for Electronics and Photonics Technology, King Abdulaziz City for Science and Technology, Riyadh, Saudi Arabia*
[3]*Computer Department, College of Science of Bizerte, Carthage University, Tunis, Tunisia*

Correspondence should be addressed to Khaled Issa; kissa@ksu.edu.sa

Received 12 August 2017; Revised 10 November 2017; Accepted 19 November 2017; Published 28 December 2017

Academic Editor: Luciano Tarricone

A novel compact dual-polarized-spectral-signature-based chipless radio-frequency identification (RFID) tag is presented. Specifically, an *L*-shape resonator-based structure is optimized to have different spectral signatures in both horizontal and vertical polarizations, in order to double the encoding capacity. Resonators' slot width and the space between closely placed resonators are also optimized to enhance the mutual coupling, thereby helping in achieving high-data encoding density. The proposed RFID tag operates over 5 GHz to 10 GHz frequency band. As a proof of concept, three different 18-bit dual-polarized RFID tags are simulated, fabricated, and tested in an anechoic chamber environment. The measurement data show reasonable agreement with the simulation results, with respect to resonators' frequency positions, null depth, and their bandwidth over the operational spectrum.

1. Introduction

Chipless radio-frequency identification (RFID) technology has found widespread use in several applications, including identification, tracking, and sensing [1–4]. Chipless RFID tags have no electronic components for their function, and the development of such tags requires the achievement of key features, including (i) high-data encoding capacity, (ii) high-data encoding density, (iii) the least tag's orientation sensitivity, (iv) minimum reader structure complexity, and (v) low-cost printability [5, 6]. However, the available chipless RFID tags do not satisfy all these requirements simultaneously.

The chipless RFID tags have been designed using frequency-, time-, phase-, hybrid-, and image-domain-based encoding techniques [3–8]. The frequency-domain (FD) tags encode the data into the spectral domain. The presence or absence of a resonance frequency (notches or nulls) associated with high-impedance circuits called resonators or frequency-selective surfaces (FSS) is considered as a code.

The FD tags are preferred over other tags because of their simple design, higher data density, and simple reader architecture. So far, numbers of configurations for FD tags have been proposed [6, 9–13]. Among the several key performance parameters, the design of FD tags is considered to enhance the data encoding density (number of encoded bits per unit area). The FD tags are classified into two types: (i) frequency-selective filter retransmission tags, and (ii) frequency-selective surfaces (FSS) or resonators tags to directly encode the backscattered signals. The design of the later type proved to be comparatively simple and compact which can offer more data encoding bits. Chipless RFID tags are designed so as to respond to an interrogating wave, which may have vertical, horizontal, circular, or elliptical polarization. Depending on the desired application, a specific polarization can be used. Note that dual-

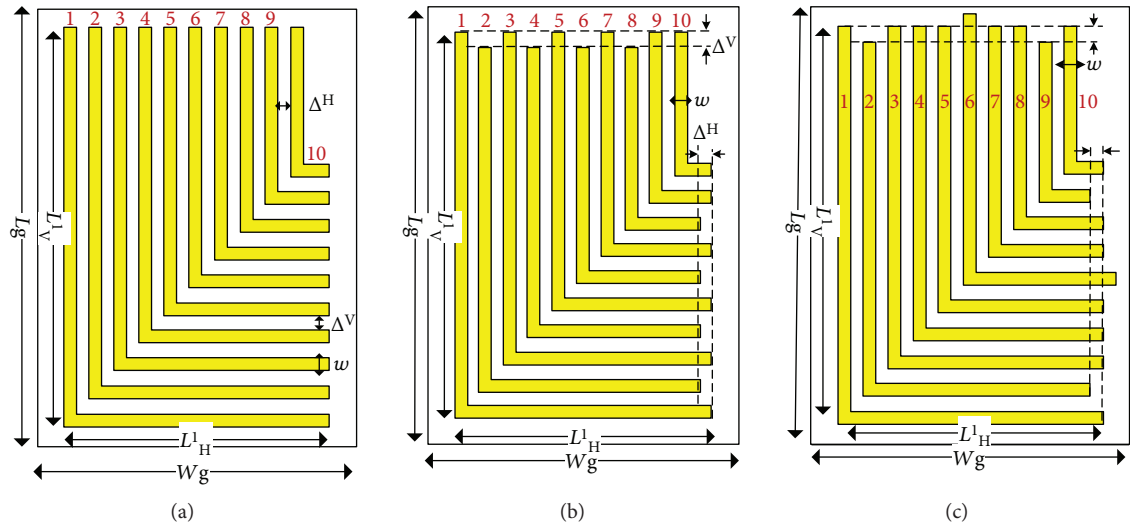

Figure 1: Structure of proposed L-shape chipless tag: (a) code 111111111, (b) code 101010101, and (c) code 101101011.

polarized tags can be of higher density (bits/cm^2) than tags insensitive to polarization [14]. However, the reader of such tags requires dual-polarized antenna and proper alignment with respect to tags' orientation [14]. An enhanced encoding capacity can be accomplished by means of the usage of two orthogonal polarizations for tag interrogation. The data encoding capacity is mainly governed by resonators' types, which are distinct from each other due to different shapes. Chipless tags having circular, square-loop-, U-, I-, V-patch-based resonators have been designed and demonstrated as FD tags [6, 9–15].

Two types of interrogation techniques are used for the FSS-based chipless tags allowing the identification or the reading of encoded data. The first is based on both a reader antenna and an interrogator antenna (bistatic measurement method). The second technique is based on a single antenna to read and interrogate (monostatic measurement method), which sends a wideband interrogation signal to read the code information. This second technique, which is the focus of our study, presents some advantages over the first technique in terms of low cost and minimum setup complexity.

In this paper, a UWB (ultra wideband) chipless RFID FD tag is presented, which encompasses novel L-shape multiresonator structure for the purpose of increasing the encoding density. According to the authors' best knowledge, the 8 bits/cm^2 encoding density presented in [15] is the largest data encoding density reported so far for monostatic FD tags. The proposed L-shape tag, on the other hand, has 12 bits/cm^2 data encoding density, that is, it has 18 bits generated by a circuit of total area of 1.5 cm^2, for the monostatic measurement setting. The L-shape has also an intrinsic flexibility that allows varying resonator's lengths both in a horizontal and a vertical direction to get an independent spectral signature in each polarization. Moreover, different codes can be generated from the optimized all-one code by simply setting two adjacent resonators to be of equal length, as will be shown later.

The proposed tag is simulated and excited as an infinite structure using floquet ports in CST simulation program. The fabricated tags are truncated in a finite 3×3 structure to develop a proof of concept circuits. The fabricated circuits have shown excellent performance having 9 bits presented by deep depth (the difference between the maximum and minimum values of a null) with values that could reach 18.15 dB over the considered spectrum. The measurements are made in an anechoic chamber with a high-gain horn antenna.

2. Proposed Chipless Tag

The proposed chipless RFID tag is displayed in Figure 1. The designed tag consists L-shape resonators. The critical design parameters $L_g, W_g, L_i^V, L_i^H, W$, Δ^V, and Δ^H are, respectively, the ground length and width, the length of ith resonator in the vertical and horizontal directions $(i = 1, 2, \ldots, N)$, slot width, and vertical and horizontal spacings.

The repetition in the L-shape resonator is made to have deep resonant notches due to the interactive interelements mutual coupling. Intrinsically, in the proposed design, the length of the horizontal/vertical patch decreases as its number increases from 1 to N. This inherently leads to the fact that the first obtained frequency null (or bit), mainly but not exclusively, corresponds to the resonance between the first and second resonators. This frequency is the lowest resonant frequency, that is, the closest to 5 GHz, and represents the lowest significant bit in the code. The proposed chipless tag is designed using single-layer copper-coated Rogger's dielectric substrate, RT/duroid® 5880, having a loss tangent of $\tan\delta = 0.002$, a dielectric constant of $\varepsilon_r = 2.2$, and a thickness of $h = 0.254$ mm.

3. Design and Optimization

The main steps summarizing the design methodology for the proposed tag are listed below.

(1) Determine the length of the ith resonator in the vertical and horizontal directions $(i = 1, 2, \ldots, N)$, according to the formulas [13]:

$$L_i^{\mathrm{V}} = \frac{c}{2f_i^{\mathrm{V}}}\sqrt{\frac{2}{1+\varepsilon_r}},$$
$$L_i^{\mathrm{H}} = \frac{c}{2f_i^{\mathrm{H}}}\sqrt{\frac{2}{1+\varepsilon_r}}, \quad (1)$$

where $f_i^{\mathrm{V}}(f_i^{\mathrm{H}})$ is the resonant frequency of the ith resonator in the vertical (horizontal) direction and c and ε_r are the speed of light and relative permittivity of the substrate, respectively. In the proposed design, f_i^{V} and f_i^{H} are separated by at least 50 MHz to achieve different coding for the vertical and horizontal polarizations. Initially, the resonant frequencies are spaced in the frequency band of interest (5–10 GHz) such that

$$f_i^{\mathrm{H}} = 5\,\mathrm{GHz} + (i-1)\times 0.5\,\mathrm{GHz},$$
$$f_i^{\mathrm{V}} = 5.05\,\mathrm{GHz} + (i-1)\times 0.5\,\mathrm{GHz}. \quad (2)$$

For N numbers of resonators, there would be N–1 notches. The jth notch $(j = 1, 2, \ldots, N-1)$ will lie between the frequencies $f_j^{\mathrm{V}}(f_j^{\mathrm{H}})$ and $f_{j+1}^{\mathrm{V}}(f_{j+1}^{\mathrm{H}})$. The N resonators are arranged so that their ends are terminated vertically and horizontally at the same level (see Figure 1(a)). This, in turn, will result in different spacings between resonators in the vertical (horizontal) direction. In what follows, the term $\Delta_{j,j+1}^{\mathrm{V}}(\Delta_{j,j+1}^{\mathrm{H}})$ is used to denote the spacing between the jth and $(j+1)$th resonators in the vertical and horizontal directions $(j = 1, 2, \ldots, N-1)$.

(2) Set all resonators to have the same slot width, W. Also, set $\Delta_{j,j+1}^{\mathrm{V}}(\Delta_{j,j+1}^{\mathrm{H}}) = \Delta_{1,2}^{\mathrm{V}}(\Delta_{1,2}^{\mathrm{H}}) = \Delta^{\mathrm{V}}(\Delta^{\mathrm{H}})$ for $j = 2, 3, \ldots, N-1$and then adjust the length of each resonator so that $L_{i+1}^{\mathrm{V}}(L_{i+1}^{\mathrm{H}}) = L_1^{\mathrm{V}}(L_1^{\mathrm{H}})$ for $i = 2, 3, \ldots, N-1$.This, in turn, will result in the design of an all-one tag. Since the aim is to have a compact size chipless RFID tag, it is required that the slot width and slot spacing are optimized so that they have the minimum possible values without compromising the desired results.

(3) Set the length of the kth resonator to the value of $L_k^{\mathrm{V}} + \Delta^{\mathrm{V}}$ (or $L_k^{\mathrm{V}} - \Delta^{\mathrm{V}}$) for the vertical polarization and $L_k^{\mathrm{H}} + \Delta^{\mathrm{H}}$ (or $L_k^{\mathrm{H}} - \Delta^{\mathrm{H}}$) for the horizontal polarization $(k = 2, 3, \ldots, N)$ so that the $(k$–1)th/kth notch gets removed, that is, different codes can be generated from the optimized all-one code by simply setting two adjacent resonator lengths to be equal. For example, Figures 1(b) and 1(c) show the tag's structures for the codes 101010101 and 101101011 in horizontal and vertical polarizations, respectively.

4. Simulation Results

A full-wave simulation was performed to design three different tags with 8, 9, and 10 resonators. These tags and their corresponding responses present 7, 8, and 9 nulls, respectively. We noted that variations in slot spacing affect the resonant frequencies and notch depths. Upon decreasing the slot spacing, there is a general behavior of upward shifts in higher resonant frequencies and vice versa. This feature of proposed structure can be used to develop different tags exhibiting different spectral signatures. Figure 2 shows the spectral response/signature of the three resonators when all-one tags are considered. By virtue of Figure 2, introducing additional resonators results in a shift in resonance frequency of their respective bits due to mutual coupling. The notch bandwidth at a particular frequency, however, remains almost the same regardless of the number of resonators.

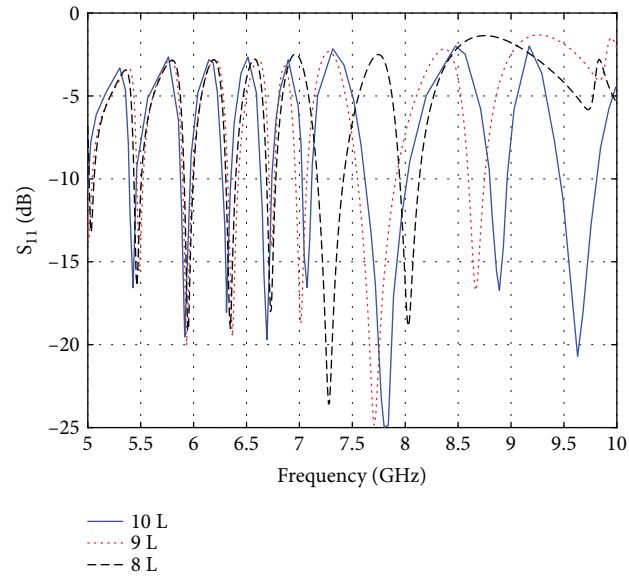

Figure 2: Responses of the three tags having 8 (dotted), 9 (dashed), and 10 (continuous) resonators.

Table 1: Design parameters.

Parameter	L_g	W_g	L_1^{H}	L_1^{V}	Δ^{H}	Δ^{H}	W
Value (mm)	15	10	9	14	0.31	0.34	0.38

Table 1 gives the values of design parameters of the tag with 10 resonators, and Figure 3(a) presents the variation of backscattered signals versus frequency from 5 to 10 GHz under vertical and horizontal polarization excitations for the all-one tag.

For each polarization, the proposed tag exhibits nine bits shown by deep nulls for both polarizations. The proposed design achieves minimum to maximum null depths, for different bits, varying from 9.6 dB to 18.15 dB, respectively. Furthermore, the bandwidth of different bits varies from 0.5 GHz up to 0.98 GHz for lower and higher order bits, respectively. The minimum and maximum frequency shift among the bits for the orthogonal polarizations ranges between 12 and 200 MHz, respectively. Figure 3(b), on the other hand, shows the response of another tag having alternating zeros and ones. Figure 3(c) also shows the response of the code 101101011. For comparison purposes, Table 2 reports

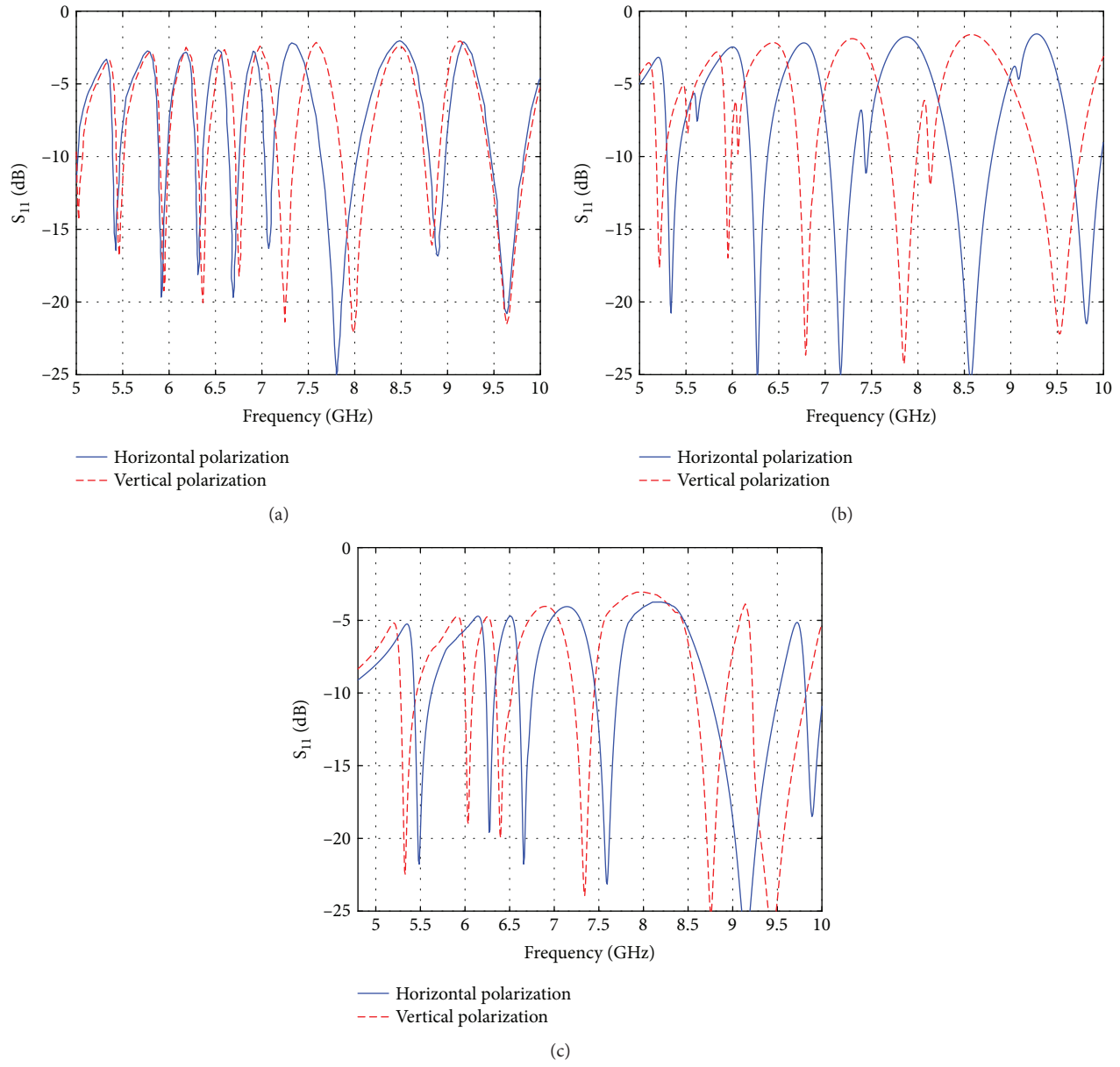

Figure 3: Tag response under horizontal and vertical excitations for optimized design: (a) code 111111111, (b) code 101010101, and (c) code 101101011.

Table 2: Comparison of different chipless RFID tags for monostatic measurement.

Resonator type	Density (bits/cm^2)	Freq. range (GHz)
Nested loops [15]	8	3–9
Stepped impedance [16]	7.9	3.1–10.6
Multiple resonators [17]	0.302	3.1–10.6
Cross loop [18]	1.25	3.1–10.1
This work	**12**	**4.8–10**

the encoding data density (number of bits/area (cm^2)) for various chipless RFID tags available in literature, which follow the same design approach presented in this work. It is clear that the proposed design outperforms the previously reported results, in terms of data density. This may be attributed to the shape of the resonators, which allows dual polarization encoding and provides flexibility to reduce size by controlling the spacing between resonators.

5. Experimental Results

For demonstration purposes, the all-one code, 101010101 code, and the 101101011 code are selected for fabrication and demonstration. The fabricated all-one code tag is shown in Figure 4(a), and the other two codes are in Figures 5(d) and 5(e). The response of the tag has been measured using UWB horn antenna operating from 1 to 18 GHz having gain values from 7 dBi up to 12 dBi. The measurements have been

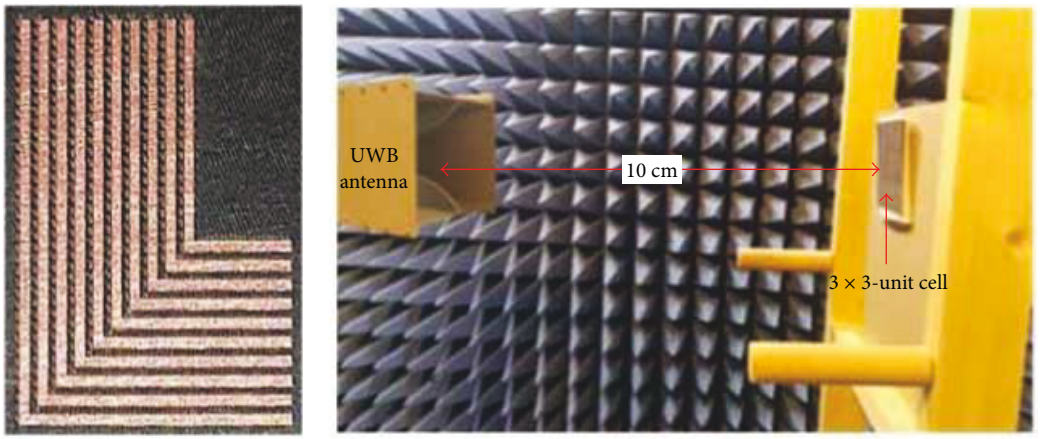

(a) (b)

Figure 4: (a) Fabricated chipless tag and (b) the experimental setup.

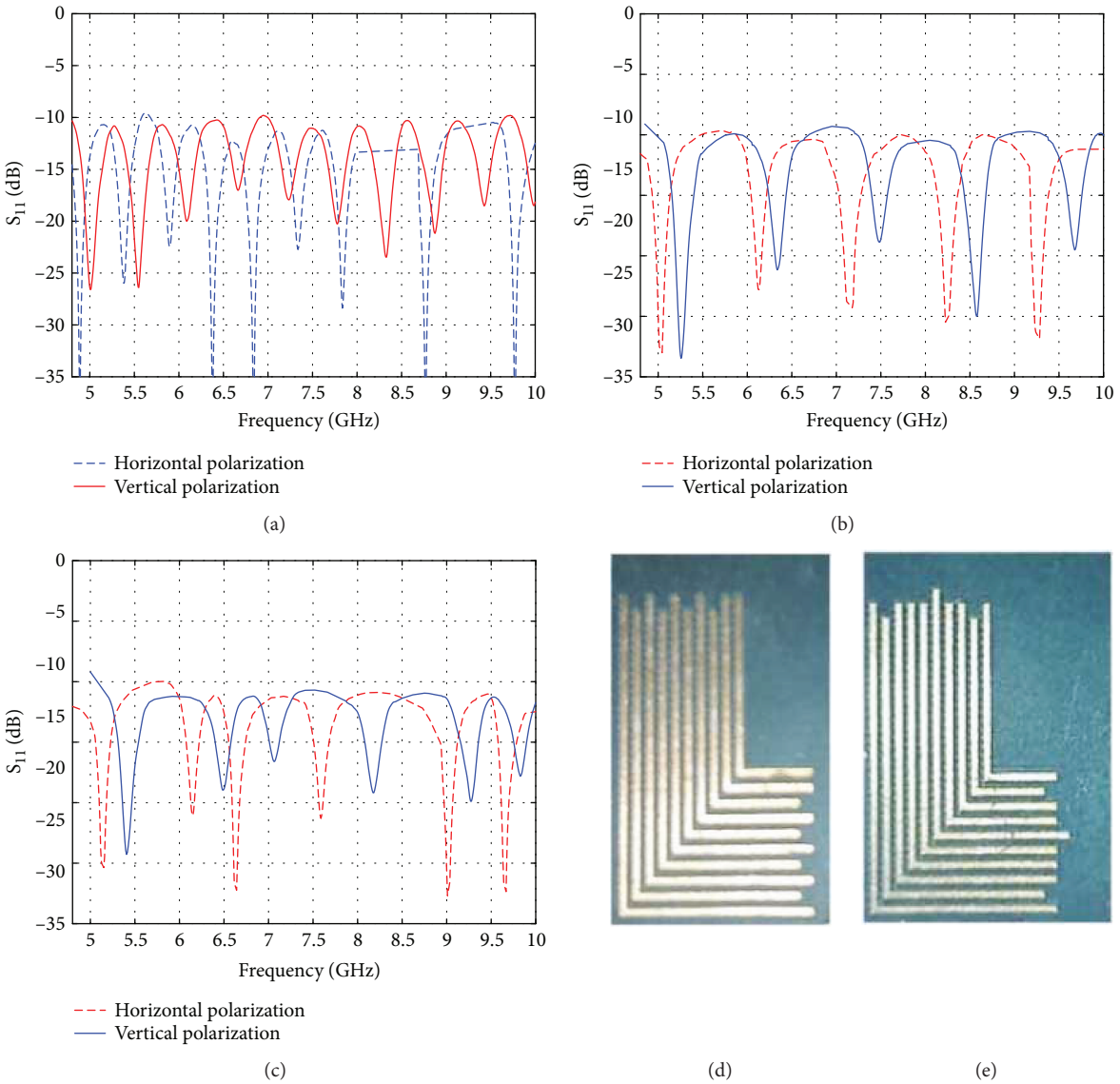

Figure 5: Measured response under horizontal and vertical excitations at 10 cm (a) ID: 111111111, (b) ID:101010101, (c) ID:101101011, (d) fabricated chipless tag ID 101010101 and, (e) fabricated chipless tag ID 101101011.

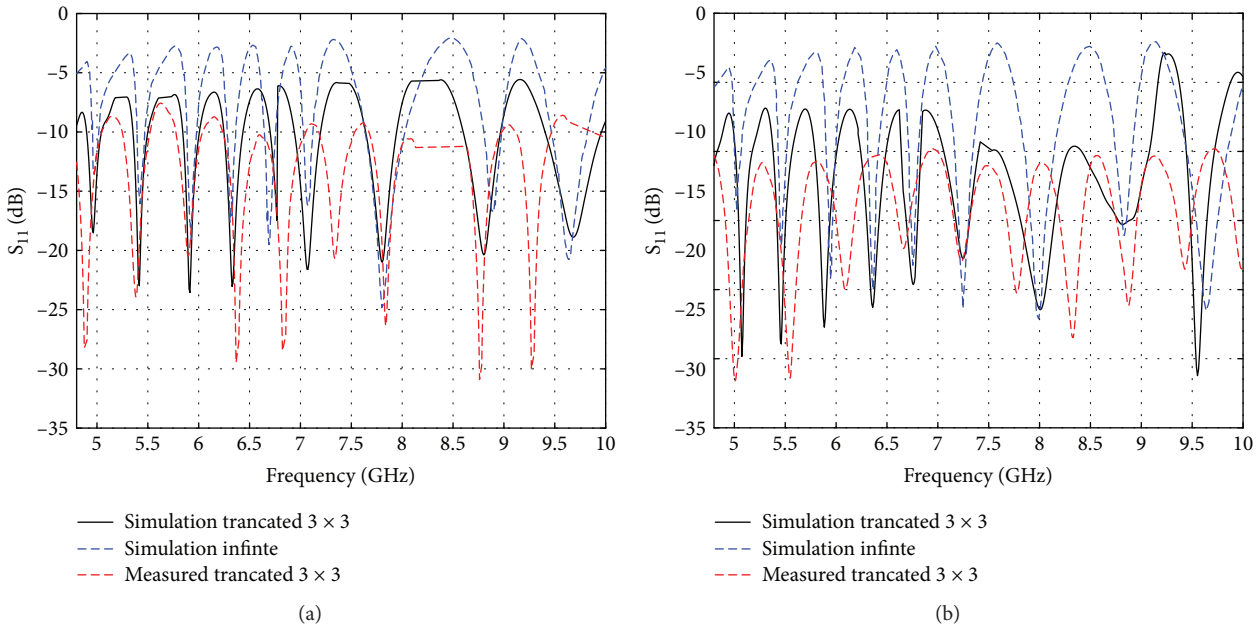

Figure 6: Simulated and measured responses of code 111111111 under (a) horizontal and (b) vertical excitations at 10 cm.

conducted in an anechoic chamber environment where the tag was placed at a distance of 10 cm from the reading antenna (see Figure 4(b)).

Figures 5(a)–5(c) present the measured responses of the L-shape chipless RFID tags under vertical and horizontal polarization excitations over the desired spectrum. The measured results show the presence of nine nulls for each polarization in the same frequency band (4.8 to 10 GHz). The backscattered signature illustrates a null depth varying between 11 dB to 22.5 dB and from 7 dB to 16 dB for horizontal and vertical polarizations, respectively. Moreover, the null bandwidth is smaller than 220 MHz for all bits and it can reach 678 MHz for the 101101011 code.

Figures 6(a) and 6(b) depict the measured (dashed) and simulated (continuous line) tag responses under horizontal and vertical polarizations, respectively. The measured results show reasonable agreement with simulation performance except for a small shift in frequency with a maximum of 278 MHz. The shift in frequency might be due to fabrication tolerance.

Moreover, the simulation results pertain to infinite structures and the measured response corresponds to a truncated finite periodic surface of a 3×3 unit cell, which could bring about a frequency shift [19]. Note that the peaks of measured response are less than those of simulated response by about 5 dB in both polarizations. Figure 7 shows tag's responses at different distances. Note that the response deteriorates after 15 cm, from which we can infer that 15 cm can reasonably be considered the reading distance in this experimental setting.

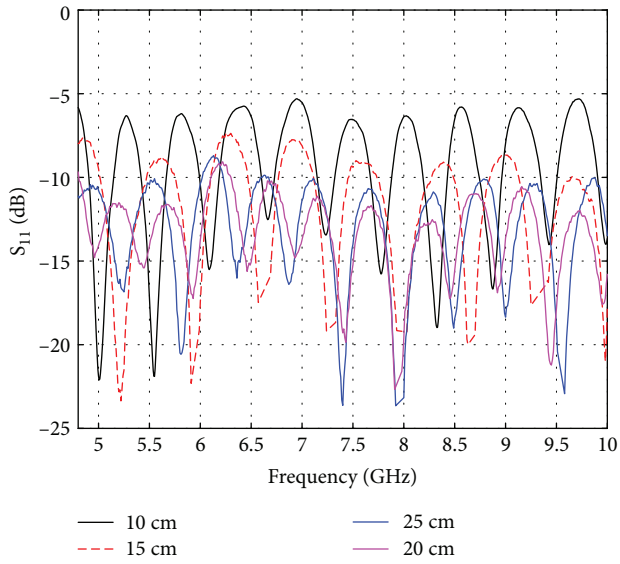

Figure 7: Measured tag's response under horizontal excitations and different distances 10, 15, 20, and 25 cm.

6. Conclusions

In this work, a monolayer chipless RFID tag operating from 5 to 10 GHz is presented. L-shape resonators are introduced to increase bit encoding capacity over a unit area. The proposed structure achieved 12 bits/cm^2 which, to the best of our knowledge, is the largest encoding density of an FD RFID tag reported in literature for monostatic measurements. The key performance parameters are optimized with several full-wave simulations, to have sharp resonant notches of 18 dB depth, with maximum 200 MHz bandwidth. The proposed L-shape FD tag operates over 5 GHz (4.8–9.8 GHz). The studied circuit is optimized by considering an infinite periodic structure. However, the fabricated circuit is truncated to a 3×3 unit cell which caused a small shift in frequency response with respect to the measured data. The

simulation performance goes in reasonable accordance with the measured performance. The proposed FD tag has encoding capability in both horizontal and vertical polarizations.

Conflicts of Interest

The authors declare no conflict of interest.

Acknowledgments

The authors extend their appreciation to the Deanship of Scientific Research at King Saud University for funding this work through no. RG-1438-092.

References

[1] E. Perret, *Radio Frequency Identification and Sensors from RFID to Chipless RFID*, John Wiley and Sons, Hoboken, NJ, USA, 2014.

[2] S. Preradovic and N. C. Karmakar, "Chipless RFID: bar code of the future," *IEEE Microwave Magazine*, vol. 11, no. 7, pp. 87–97, 2010.

[3] M. Popperl, A. Parr, C. Mandel, R. Jakoby, and M. Vossiek, "Potential and practical limits of time-domain reflectometry chipless rfid," *IEEE Transactions on Microwave Theory and Techniques*, vol. 64, no. 9, pp. 2968–2976, 2016.

[4] M. M. Khan, F. A. Tahir, M. Farooqui, A. Shamim, and H. M. Cheema, "3.56-bits/cm^2 compact inkjet printed and application specific chipless rfid tag," *IEEE Antennas and Wireless Propagation Letters*, vol. 15, pp. 1109–1112, 2016.

[5] A. Habib, Y. Amin, M. A. Azam, J. Loo, and H. Tenhunen, "Frequency signatured directly printable humidity sensing tag using organic electronics," *IEICE Electronics Express*, vol. 14, no. 3, pp. 20161081–22016108, 2017.

[6] S. Preradovic, I. Balbin, N. C. Karmakar, and G. F. Swiegers, "Multiresonator-based chipless RFID system for low-cost item tracking," *IEEE Transactions on Microwave Theory and Techniques*, vol. 57, no. 5, pp. 1411–1419, 2009.

[7] A. Vena, E. Perret, and S. Tedjini, "Chipless rfid tag using hybrid coding technique," *IEEE Transactions on Microwave Theory and Techniques*, vol. 59, no. 12, pp. 3356–3364, 2011.

[8] A. Lazaro, A. Ramos, D. Girbau, and R. Villarino, "Signal processing techniques for chipless UWB RFID thermal threshold detector detection," *IEEE Antennas and Wireless Propagation Letters*, vol. 15, pp. 618–621, 2016.

[9] S. Shrestha, M. Balachandran, M. Agarwal, V. V. Phoha, and K. Varahramyan, "A chipless RFID sensor system for cyber centric monitoring applications," *IEEE Transactions on Microwave Theory and Techniques*, vol. 57, no. 5, pp. 1303–1309, 2009.

[10] A. Lazaro, A. Ramos, D. Girbau, and R. Villarino, "Chipless UWB RFID tag detection using continuous wavelet transform," *IEEE Antennas and Wireless Propagation Letters*, vol. 10, pp. 520–523, 2011.

[11] R. Rezaiesarlak and M. Manteghi, "Complex-natural-resonance-based design of chipless rfid tag for high-density data," *IEEE Transactions on Microwave Theory and Techniques*, vol. 62, pp. 898–904, 2014.

[12] K. V. S. Rao, P. V. Nikitin, and S. F. Lam, "Antenna design for UHF RFID tags: a review and a practical application," *IEEE Transactions on Antennas and Propagation*, vol. 53, no. 12, pp. 3870–3876, 2005.

[13] T. Dissanayake and K. P. Esselle, "Prediction of the notch frequency of slot loaded printed UWB antennas," *IEEE Transactions on Antennas and Propagation*, vol. 55, no. 11, pp. 3320–3325, 2007.

[14] S. H. Zainud-Deen, M. A. Abo-Elhassan, H. A. Malhat, and K. H. Awadalla, "Dual-polarized chipless RFID tag with temperature sensing capability," in *2014 31st National Radio Science Conference (NRSC)*, Cairo, Egypt, 2014.

[15] F. Costa, S. Genovesi, and A. Monorchio, "Normalization-free chipless RFIDs by using dual-polarized interrogation," *IEEE Transactions on Microwave Theory and Techniques*, vol. 64, no. 1, pp. 310–318, 2016.

[16] C. M. Nijas, U. Deepak, P. Vinesh et al., "Low-cost multiple-bit encoded chipless rfid tag using stepped impedance resonator," *IEEE Transactions on Antennas and Propagation*, vol. 62, no. 9, pp. 4762–4770, 2014.

[17] L. Das, T. Riny, M. N. Chakkanattu, M. Pezholil, A. Novel Polarization, and R. F. I. D. Independent Chipless, "Tag using multiple resonators," *Progress in Electromagnetics Research Letters*, vol. 55, pp. 61–66, 2015.

[18] V. Sajitha, C. M. Nijas, T. Roshna, K. Vasudevan, and P. Mohanan, "Compact cross loop resonator based chipless rfid tag with polarization insensitivity," *Microwave and Optical Technology Letters*, vol. 58, no. 4, pp. 944–947, 2016.

[19] F. Costa, S. Genovesi, and A. Monorchio, "A chipless RFID based on multiresonant high-impedance surfaces," *IEEE Transactions on Microwave Theory and Techniques*, vol. 61, no. 1, pp. 146–153, 2013.